Anal Bioanal Chem
DOI 10.1007/s00216-016-9472-5

RESEARCH PAPER

Fluorescent biosensor for the detection of hyaluronidase: intensity-based ratiometric sensing and fluorescence lifetime-based sensing using a long lifetime azadioxatriangulenium (ADOTA) fluorophore

Rahul Chib[1] · Mark Mummert[2] · Ilkay Bora[3] · Bo W. Laursen[3] · Sunil Shah[1] · Robert Pendry[4] · Ignacy Gryczynski[1] · Julian Borejdo[1] · Zygmunt Gryczynski[1,4] · Rafal Fudala[1]

Received: 21 December 2015 / Revised: 22 February 2016 / Accepted: 7 March 2016

Abstract In this report, we have designed a rapid and sensitive, intensity-based ratiometric sensing as well as lifetime-based sensing probe for the detection of hyaluronidase activity. Hyaluronidase expression is known to be upregulated in various pathological conditions. We have developed a fluorescent probe by heavy labeling of hyaluronic acid with a new orange/red-emitting organic azadioxatriangulenium (ADOTA) fluorophore, which exhibits a long fluorescence lifetime (~20 ns). The ADOTA fluorophore in water has a peak fluorescence lifetime of ~20 ns and emission spectra centered at 560 nm. The heavily ADOTA-labeled hyaluronic acid (HA-ADOTA) shows a red shift in the peak emission wavelength (605 nm), a weak fluorescence signal, and a shorter fluorescence lifetime (~4 ns) due to efficient self-quenching and formation of aggregates. In the presence of hyaluronidase, the brightness and fluorescence lifetime of the sample increase with a blue shift in the peak emission to its original wavelength at 560 nm. The ratio of the fluorescence intensity of the HA-ADOTA probe at 560 and 605 nm can be used as the sensing method for the detection of hyaluronidase. The cleavage of the hyaluronic acid macromolecule reduces the energy migration between ADOTA molecules, as well as the degree of self-quenching and aggregation. This probe can be efficiently used for both intensity-based ratiometric sensing as well as fluorescence lifetime-based sensing of hyaluronidase. The proposed method makes it a rapid and sensitive assay, useful for analyzing levels of hyaluronidase in relevant clinical samples like urine or plasma.

Keywords Hyaluronidase sensing · Azadioxatriangulenium fluorophore · Ratiometric sensing · Fluorescence lifetime-based sensing · Fluorescence-based assay

Electronic supplementary material The online version of this article (doi:10.1007/s00216-016-9472-5) contains supplementary material, which is available to authorized users.

✉ Rahul Chib
rc0307@live.unthsc.edu

✉ Rafal Fudala
Rafal.Fudala@unthsc.edu

[1] Department of Cell Biology, Immunology and Microbiology, Center for Fluorescence Technologies and Nanomedicine, University of North Texas Health Science Center, Fort Worth, TX 76107, USA

[2] Mental Sciences Institute, University of North Texas Health Science Center, Fort Worth, TX 76107, USA

[3] Nano-Science Center & Department of Chemistry, University of Copenhagen, Universitetsparken 5, 2100 København Ø, Denmark

[4] Department of Physics and Astronomy, Texas Christian University, Fort Worth, TX 76129, USA

Introduction

Hyaluronidase is a family of endoglycosidase that catalyzes the depolymerization of hyaluronic acid (HA) via cleavage of β-*N*-acetyl-D-glucosaminidic bonds [1]. Hyaluronidase is known to be involved in various physiological and pathological conditions like fertilization, embryogenesis, inflammation, tumor growth, and wound healing [2–6]. Initially in the literature, it was described as a "spreading factor" which was found in the testicular extract of animal and humans. It was later characterized as hyaluronic acid-degrading enzyme and called hyaluronidase [5, 7–9]. Recent studies have shown the role of hyaluronic acid and hyaluronidase with the

Published online: 18 March 2016

differentiation, proliferation, migration, and angiogenesis of tumor cells [2, 10, 11]. HA is a linear, non-sulfated glycosaminoglycan composed of multiple subunits of D-glucuronic acid and *N*-acetylglucosamine. In humans, HA is known to maintain various important functions like cartilage integrity, osmotic balance, and homeostasis of water owing to its gel-like properties [12–14]. An overexpression of hyaluronidase is associated in the literature with patients suffering from cancers, such as prostate cancer [15], bladder cancer [6], head and neck carcinoma [4], colon cancer, and malignant melanoma [5]. Therefore, it is of great interest to develop a simple, sensitive, and fast technique with which one can estimate the activity/level of hyaluronidase in biological samples.

Several methods have been reported in the literature for detecting hyaluronidase activity, which mainly depends on the degradation of hyaluronic acid by hyaluronidase. To measure hyaluronidase activity/level, there are several methods reported in the literature which includes turbidimetry [16], viscometry [17], ELISA-like assay [18, 19], colorimetry [20], zymography [21, 22], and fluorescence detection [23–32]. Methods like turbidimetry, colorimetry, and viscometry are not very sensitive and cannot detect the level of hyaluronidase at different time points of an experiment. Zymography is simple yet not very sensitive for quantitative measurements. ELISA-like assays are sensitive and selective but do not allow real-time monitoring of hyaluronidase activity. However, fluorescence-based detection of hyaluronidase is a fast and sensitive method, useful for high-throughput screening, and has a real-time monitoring capability and their usefulness in biological samples makes it an ideal method for hyaluronidase detection.

Various novel fluorescence assays designed to detect hyaluronidase activity have been reported in the literature. These fluorescent probes have been designed for hyaluronidase detection by using hyaluronic acid as a template and labeling it with gold nanoparticles [23, 33], organic fluorescent dyes [34, 35], conjugated small molecules [36], and upconversion luminescence material [29]. Although these fluorescence-based methods have superior properties compared to previous methods in terms of sensitivity, they also have a few drawbacks. For example, gold nanoparticles precipitate in biological high salt environments [26, 37]. Fluorescent probes developed using organic fluorophores are smaller in size compared to probes developed using quantum dots, nanodots, and noble metal nanoparticle as the luminescent material. Some fluorescent probes have a very short fluorescence lifetime and hence cannot be used for lifetime-based sensing or imaging, as the background of the biological sample interferes with the fluorescence signal of the probe and cannot be easily removed as the fluorescence intensity decay of background and probe is almost similar [27, 34].

To make this probe, we heavily labeled hyaluronic acid with an azadioxatriangulenium (ADOTA) fluorophore. ADOTA is an orange/red-emitting organic fluorophore with peak emission centered at 560 nm and a fluorescence lifetime of 20 ns in aqueous solution. Our previous studies have shown that it is the only red-emitting organic fluorophore with a long fluorescence lifetime of 20 ns [38–47]. One major problem encountered using fluorescence detection methods in biological fluids, cells, and tissue is the presence of autofluorescence which reduces the obtainable signal-to-noise ratio. As most biomolecules emit at higher energies, the autofluorescence level decreases towards the red/NIR region of the electromagnetic spectrum. Therefore, using a red-emitting fluorophore can help to overcome this issue.

The goal of this study was to develop a rapid and sensitive ratiometric sensing probe for estimating hyaluronidase activity/level. To achieve this goal, a simple strategy was used where we developed a probe using HA as template and labeled it with an orange/red-emitting organic fluorophore with a long fluorescence lifetime. The design of this probe was created by heavy labeling of HA with an aniline-substituted ADOTA fluorophore (Scheme 1) [48]. When a certain molar ratio of the fluorophore to hyaluronic acid is reached, fluorophores are close enough that dimers or higher order aggregates may form. The aggregated dyes display red-shifted absorption and fluorescence as well as reduced fluorescence lifetime (4 ns). Even a small fraction of aggregates dominates the optical properties due to the close proximity of all dyes bound to HA and the resulting quenching of non-aggregated dyes via energy transfer to the red-shifted aggregates. The fluorescence intensity and fluorescence lifetime of the HA-ADOTA probe are thus significantly reduced compared to the non-aggregated ADOTA dye. The fluorescence signal will recover after the degradation of the probe by hyaluronidase, where the long hyaluronic acid chains of the HA-ADOTA probe are split into shorter fragments and the fluorophore molecules will move apart. It was observed from our previous observations that the aggregation of ADOTA fluorophore causes a red shift in the peak emission wavelength [38]. Similarly, heavy labeling of hyaluronic acid with ADOTA causes a shift in the peak emission wavelength of the probe to 605 nm. Once the hyaluronidase starts degrading this probe, the peak emission wavelength shifts back to its original position at 560 nm. This shift in emission wavelength after degradation of the probe provides a method to develop a ratiometric sensing probe, where the ratio of emission intensity of the digested to undigested probe can be used to calculate hyaluronidase activity/level. Some of the reported methods for the fluorescence detection utilize single fluorescence intensity as the sensing method. Collection of the signal at a fixed wavelength can be tempered due to various reasons like fluctuation in the excitation intensity, emission collection efficiency, change in focal point, etc.[49, 50]. These problems can be overcome by ratiometric collection of signal at two different wavelengths. Ratiometric sensing acts in a self-

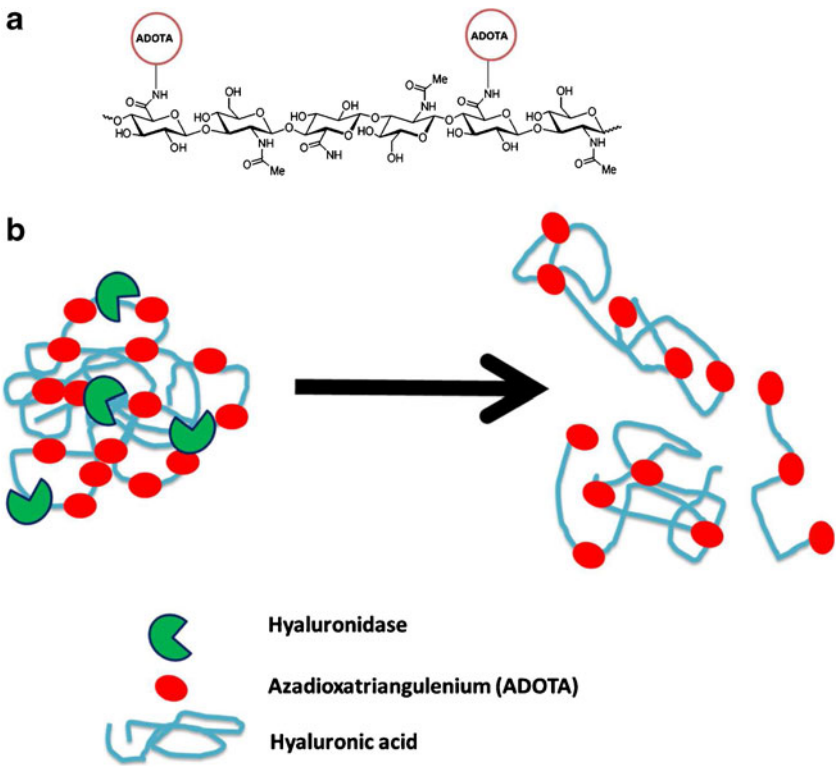

Scheme 1 Schematic representation for the assay system and its response to the enzyme hyaluronidase. (**A**) Covalent binding of ADOTA fluorophore to the COOH group of hyaluronic acid. (**B**) Undigested HA-ADOTA probe and cleaved probe following enzymatic action

calibrating way to minimize interfering factors while allowing for more accurate detection of analyte [51–53].

The activity/level of hyaluronidase can also be estimated using the change in the fluorescence lifetime of the biosensor as the aggregation in the undigested probe leads to a decrease in the fluorescence lifetime (4 ns). After cleavage of the biosensor by hyaluronidase, a recovery in the amplitude-weighted fluorescence lifetime was observed (15 ns). This large difference in the fluorescence lifetime of the probe can be used for the detection of hyaluronidase. Here in this paper, we tested the HA-ADOTA probe in spiked PBS and we also used it to measure hyaluronidase activity/level in cell culture media from a prostate cancer cell line (DU-145) which is known to express higher levels of hyaluronidase [15, 54].

Materials and methods

Sodium hyaluronate from bacterial fermentation was obtained from Acros Organics (Thermo Fisher Scientific, Fair Lawn, NJ). Dimethyl sulfoxide (DMSO), guanidine hydrochloride, acetaldehyde, cyclohexyl isocyanide, centricon filter (30,000 molecular cutoff), and bovine testis hyaluronidase (EC 3.2.1.35, type 1-S, 451 U/mg) were obtained from Sigma-Aldrich (Sigma-Aldrich, St. Louis, MO). Dulbecco's phosphate-buffered saline (PBS), fetal bovine serum (FBS), DMEM media, antibiotic, insulin, transferrin, and selenium (ITS) supplement, and Slide-A-Lyser dialysis cassettes (10, 000 molecular weight cutoff) were purchased from Thermo Fisher Scientific (Waltham, MA). ELISA kit for hyaluronic acid was purchased from R&D Systems (Minneapolis, MN). DU-145 cells were purchased from ATCC (Manassas, VA). The ADOTA fluorophore (*N*-(4-aminophenyl)-azadioxatriangulenium tetrafluoroborate) was synthesized as described elsewhere [48]. All compounds, solvents, and materials were used as received; water was used directly from a Millipore (Billerica, MA) purification system.

Preparation of the active amine form of the azadioxatriangulenium (ADOTA-NH_2) fluorophore

The ADOTA fluorophore with a reactive amine group was prepared according to previously published procedures [48]. Briefly, tris(2,6-dimethoxyphenyl)methylium tetrafluoroborate was reacted with *p*-aminoaniline and 2,6-lutidinein acetonitrile at ambient temperature for 90 min to form the respective acridinium salt. Subsequent twofold ring closure in molten pyridinium hydrochloride at 200 °C in 60 min provided the fluorescent ADOTA. Precipitation as the tetrafluoroborate salt and recrystallization from methanol yield the pure compound in excellent yield as dark crystals (Scheme 2).

Preparation of HA-ADOTA probe

The starting material for the preparation of the reactive amine of the AzaDiOxaTriaAngulenium (ADOTA-phenyl-NH_2)

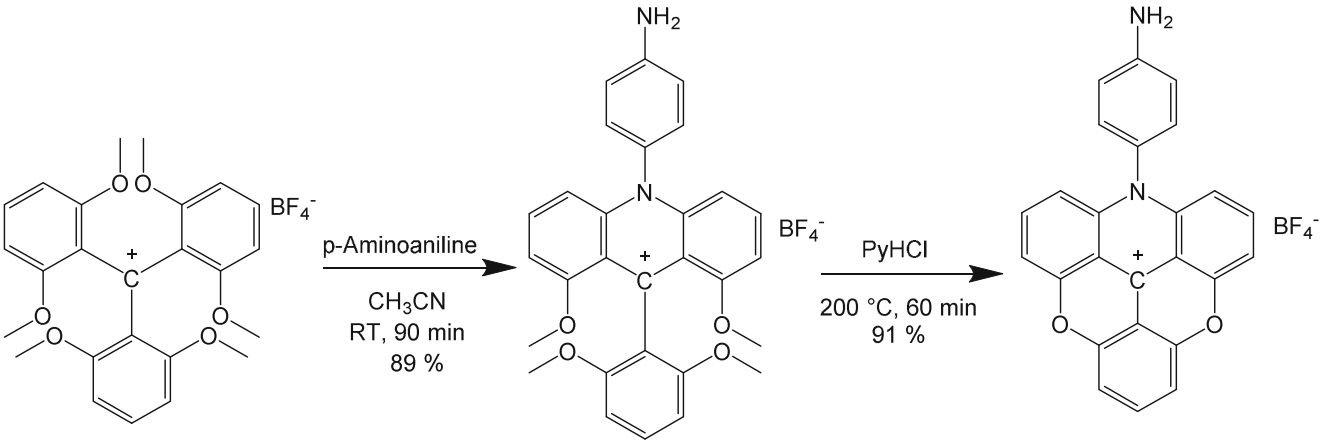

Scheme 2 Synthetic procedure for the preparation of *p*-aminophenyl-ADOTA BF_4

was prepared according to the above-described method (Scheme 2). HA was dissolved to 1.25 mg/mL in dH_2O and then diluted 1:2 in DMSO. The ADOTA-NH_2 was dissolved in DMSO and added to the HA solution for a final ADOTA-NH_2 concentration of 25 mg/mL. Acetaldehyde and cyclohexyl isocyanide were added to 0.04 % (*v*/*v*), and the reaction was allowed to proceed for 48 h at 25 °C. Afterwards, the solution was diluted 1:14 in ethanol/guanidine HCl (50 μL of 3 M guanidine HCl per 900 μL of 100 % ethanol) and the HA-ADOTA allowed to precipitate overnight at −20 °C. The precipitate was then dissolved in 1 mL of dH_2O followed by extensive dialysis against dH_2O. The concentration of HA in the probe was measured using ELISA kit for hyaluronic acid and was found to be 0.6 mg/mL.

Preparation of cell culture media

Concentrated cell culture media were prepared according to the method mentioned by Lokeshwar et al. with slight modifications [54]. DU-145 cells were plated in DMEM media containing 10 % FBS and 1 % antibiotic solution. After 70 % confluency, cells were washed three times with serum-free DMEM media. Cells were then incubated with serum-free DMEM media with ITS supplement. The serum-free media were collected after 72 h and concentrated ten times using 30,000 molecular cutoff centricon filter. Concentrated media from six culture flasks were pooled together and used for analyzing hyaluronidase activity in the media.

Experimental section

Absorption measurements

Absorption spectra were measured using a Cary 50 Bio UV–visible spectrophotometer (Varian Inc., Australia). Absorption spectra were scanned from 350 to 620 nm in PBS at room temperature.

Steady-state fluorescence measurements of hyaluronan hydrolysis

The HA-ADOTA probe was incubated with different amount of hyaluronidase (0–100 U/mL) in PBS, pH 7.4, at room temperature. The fluorescence emission spectra were recorded every 10 min for 150 min for all the concentrations of the enzyme. Steady-state fluorescence intensity measurements of all the samples were made using a Carry Eclipse spectrofluorometer (Varian Inc., Australia) using a 10-mm × 4-mm quartz cuvette. The emission was scanned from 520 to 700 nm following a 470-nm excitation and using a 495-nm-long pass filter on the emission side. Steady-state excitation spectra were measured by observing the emission at 605 nm, and excitation was scanned from 400 to 600 nm using a 590-nm-long pass filter on the emission side.

Fluorescence intensity decay

Same amount of HA-ADOTA probe was added to PBS (pH 7.4) with varying amount of hyaluronidase (0–100 U/mL). The change in fluorescence lifetime was measured for all the concentrations of enzyme every 20 min for 160 min. Fluorescence lifetimes of all the samples were measured using FluoTime 200 (PicoQuant, GmbH, Berlin, Germany) time-resolved spectrofluorometer. This instrument contains a multichannel plate detector (Hamamatsu, Japan), and a 470-nm laser diode was used as the excitation source. The fluorescence intensity decays were measured under magic angle conditions (54.7°), and data was analyzed with FluoFit version 4.5.3 software (PicoQuant GmbH, Berlin, Germany) using the exponential reconvolution procedure using nonlinear

regression (multiexponential deconvolution model). In the case of multiexponential analysis, the fluorescence decay was analyzed using:

$$I(t) = \sum_i \alpha_i \exp(-t/\tau_i)$$

where τ_i are the decay time and α_i are the pre-exponential factors (amplitudes) of the individual components. Amplitude-weighted lifetime is given by:

$$\langle \tau \rangle = \sum_i \alpha_i \tau_i$$

For measuring fluorescence lifetime of HA-ADOTA in solution containing concentrated media from DU-145 cells, a confocal microscope equipped with time-correlated single photon counting (TCSPC) detector was used (MicroTime 200, PicoQuant, Germany). A 470-nm laser operating at 5 MHz repetition rate was used. Sample is prepared in a glass bottom petri dish, and laser excitation is used on Olympus 1X71 inverted microscope. The signal from the detector was routed into a PicoHarp 300 (PicoQuant, Germany) TCSPC module. Fluorescence lifetime was measured every 10 min for 150 min. All analyses were performed using SymPho Time, V.5.3.2 software from PicoQuant.

Results and discussion

Scheme 1 shows the schematic representation of HA-ADOTA probe. The HA-ADOTA probe obtained from heavy labeling of ADOTA fluorophore produces a low fluorescence signal and exhibit a short fluorescence lifetime resulting from aggregation and FRET between ADOTA molecules and aggregates. Nevertheless, the addition of hyaluronidase to the HA-ADOTA biosensor solution causes a strong fluorescence enhancement and an increase in the fluorescence lifetime, which is attributed to the specific cleavage of the hyaluronic acid template by hyaluronidase and the breakup of aggregates and spatial separation of fluorophores.

Figure 1 shows the absorption spectrum of HA-ADOTA probe in PBS solution at room temperature with the maximum absorption peak centered at 540 nm. A second transition is of lower oscillator strength with peak centered at 440 nm. As it can be seen from Fig. 1, even though the main absorption peak is centered at 540 nm, a 470-nm excitation is also enough to excite the probe. Furthermore, a complete emission spectrum can be obtained when the probe is excited using a 470-nm excitation source. The concentration of the ADOTA in the stock HA-ADOTA is 13.96 μM. The probe was diluted 200 times in the assay system (70 nM).

The normalized emission spectra of HA-ADOTA probe and free ADOTA fluorophore in PBS following a 470-nm excitation are shown in Fig. 2A. It can be seen from the graph that the emission spectra of free fluorophore are centered at 560 nm, whereas the peak emission of HA-ADOTA probe is centered at 605 nm. The 45-nm shift in the peak emission wavelength was obtained due to aggregation of the fluorophore molecules. This shift in the peak emission proves the efficient energy transfer between the ADOTA molecules and in fact shows the efficient design of this biosensor.

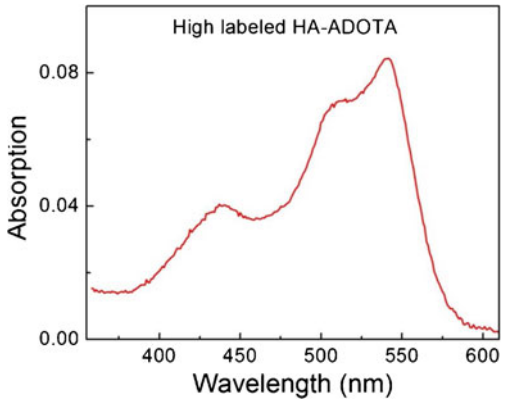

Fig. 1 The absorption spectrum of HA-ADOTA probe in PBS (pH 7.4). The concentration of ADOTA in HA-ADOTA probe is 13.96 μM. HA-ADOTA probe in the assay system is 70 nM

The excitation spectra and emission spectra of HA-ADOTA probe before and after enzymatic cleavage with 100 U/mL of hyaluronidase are shown in Fig. 2B. It can be seen from Fig. 2B that the emission spectrum of the digested probe shifts back to its original peak emission wavelength of 560 nm, whereas the intact probe has a peak emission wavelength centered at 605 nm. This aggregation-induced shift in the emission wavelength allows for an efficient method to ratiometrically detect the enzyme activity by measuring the fluorescence intensity at two wavelengths, i.e. 560 and 605 nm. The ratiometric sensing provides a built-in self-calibration and higher accuracy in terms of quantitative analysis. We also observed a small change in the excitation spectra of HA-ADOTA probe before and after cleavage by hyaluronidase. The shift in the emission wavelength of the HA-ADOTA probe is also visible to the eye. Figure 2C shows the change in the color of the solution containing HA-ADOTA probe before and after enzymatic cleavage, when excited using a handheld blue laser. We also estimated the quantum yield of the ADOTA monomer and aggregates by mimicking the monomer/aggregate system in thin polyvinyl alcohol (PVA) films with low and high concentration of ADOTA. The estimated quantum yield for monomer is 55 %, whereas the quantum yield for aggregate ADOTA system is less than 1 %. The details about quantum yield measurement are given in the Electronic Supplementary Material (ESM, Fig. S1).

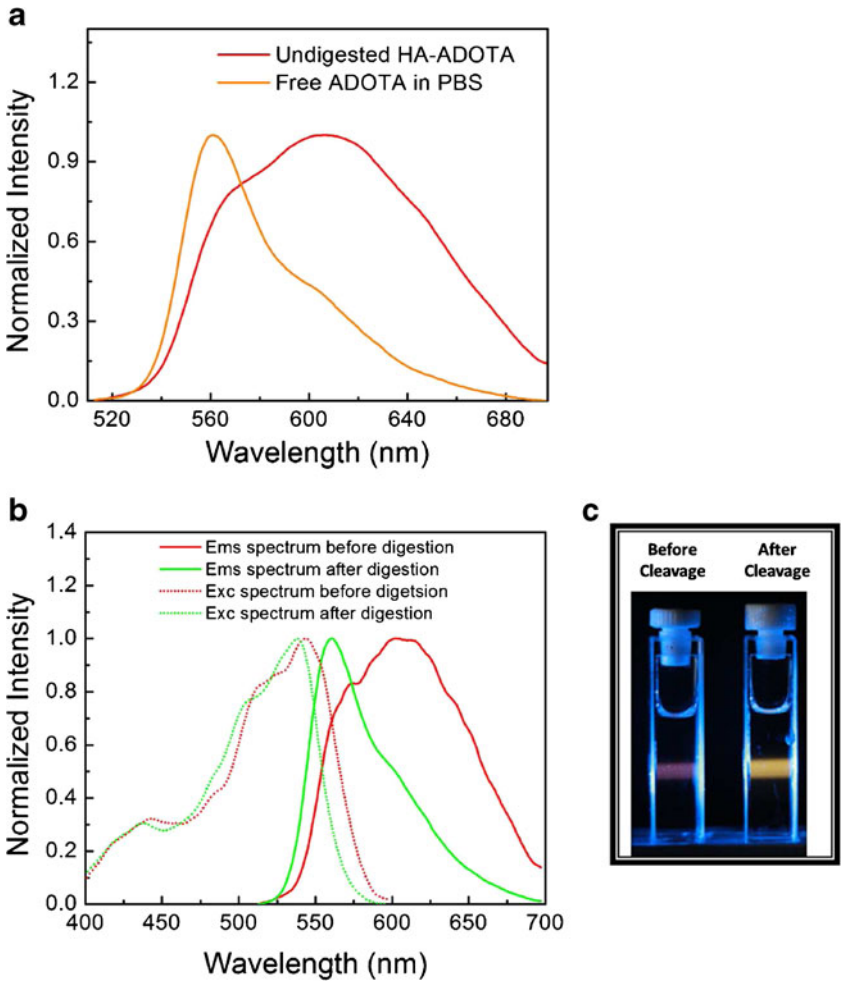

Fig. 2 (**A**) Normalized emission spectra of free ADOTA fluorophore in PBS (pH 7.4) and the emission spectra of HA-ADOTA probe (70 nM ADOTA) in PBS (pH 7.4) when excited using a 470-nm light source. (**B**) The excitation and emission spectra of heavily labeled HA-ADOTA (70 nM ADOTA) probe before and after enzymatic cleavage. The large spectral overlap between excitation and emission spectra is responsible for an efficient excitation energy migration (HOMO-FRET) between ADOTA molecules. The energy migration between ADOTA molecules is responsible for the self-quenching process. (**C**) Pictorial representation of the change in the color of HA-ADOTA solution before and after hyaluronidase cleavage

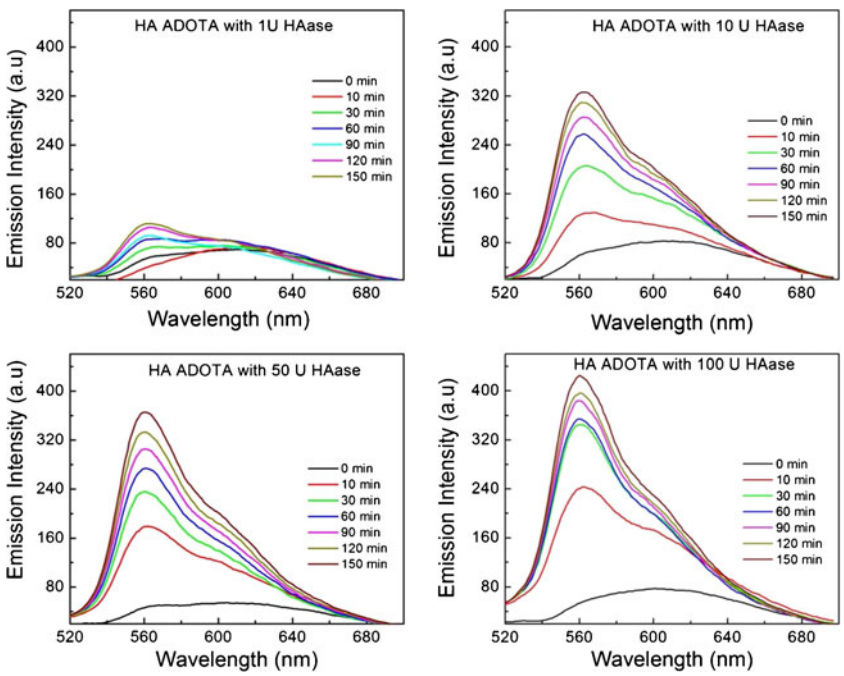

Fig. 3 The change is fluorescence emission of HA-ADOTA probe (70 nM ADOTA, PBS pH 7.4) after incubation with different amount of hyaluronidase enzyme. The fluorescence emission spectra were collected for 150 min. A 470-nm laser was used for the excitation, and the experiments were performed in triplicate and a similar increase in fluorescence intensity was observed

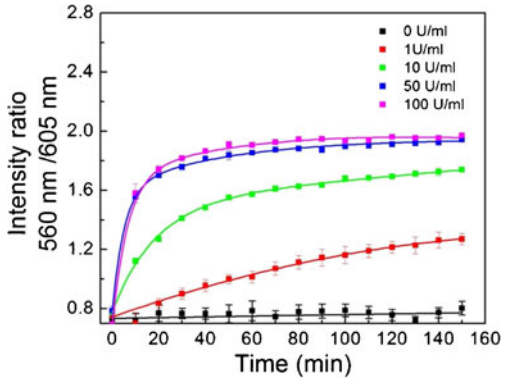

Fig. 4 Change is the ratio of emission intensity (560 nm/605 nm) of the assay system (70 nm ADOTA) in PBS buffer (PBS 7.4) at room temperature vs reaction time in the presence of different amount of hyaluronidase. A 470-nm laser was used for excitation, and all the experiments were performed in triplicate

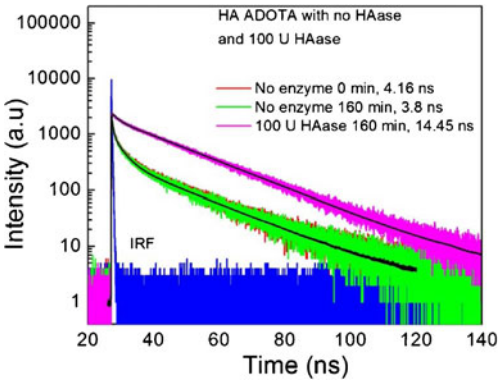

Fig. 6 The fluorescence intensity decay of HA-ADOTA probe (70 nm ADOTA, 0.6 mg/mL HA) in PBS (pH 7.4) in the absence and presence of hyaluronidase. In the presence of enzyme, an increase in the fluorescence lifetime was observed. Without the enzyme at 0 min, three components are needed to fit the data with amplitudes of 0.16, 0.53, and 0.31 with the lifetime of 18, 0.41, and 3.23 ns. With 100 U/mL of hyaluronidase at 160 min, the decay was fitted using two components with amplitudes of 0.74 and 0.26 and with lifetime of 18.85 and 1.83 ns. All fluorescence lifetime measurements were performed in triplicate

Response of HA-ADOTA probe with hyaluronidase

As mentioned, the HA-ADOTA probe was synthesized by heavy labeling of hyaluronic acid with ADOTA fluorophore through covalent bond formation. To investigate the response of the biosensor towards hyaluronidase, the fluorescence response of HA-ADOTA probe to hyaluronidase at varying concentration was investigated by adding hyaluronidase to HA-ADOTA probe (70 nM ADOTA) in PBS (pH 7.4) at room temperature. Figure 3 shows the hyaluronidase concentration-dependent change in the fluorescence intensity of the HA-ADOTA probe. The fluorescence intensity of the reaction system increases with increasing concentration of hyaluronidase from 0 to 100 U/mL of hyaluronidase. Even 1 U/mL of hyaluronidase was enough to increase the fluorescence intensity and causes the shift in the peak emission of the HA-ADOTA probe. In the case of 1 U/mL of hyaluronidase, the fluorescence intensity shows 1.7 times enhancement in the fluorescence signal, whereas, in the case of 100 U/mL of enzyme, 5.6 times enhancement in the fluorescence signal was observed. The emission intensity for different amount of hyaluronidase are drawn to the same scale so as to easily distinguish the change in the fluorescence enhancement with different amount of enzyme.

The kinetic assay of the enzymatic reaction was determined by measuring the time-dependent change in the fluorescence intensity of the HA-ADOTA probe in the absence and presence of hyaluronidase. We assessed the change in fluorescence intensity for all concentrations of enzyme every 10 min for 150 min and calculated the change in the intensity ratio using the fluorescence intensity at 560 and 605 nm as the observation points. From Fig. 4, it can be seen that in the absence of hyaluronidase, we did not notice any change in the ratio of fluorescence intensity, which proves the stability of HA-ADOTA probe. The time-dependent fluorescence intensity measurement shows that the emission intensity ratio at 560 and 605 nm gradually increases with increasing amount of enzyme and time. It was also observed from Fig. 4 that the emission intensity ratio almost reaches a plateau after 80 min of reaction when the enzyme concentration was 50 U/mL or higher. To ensure the reaction was complete, we took 100 min

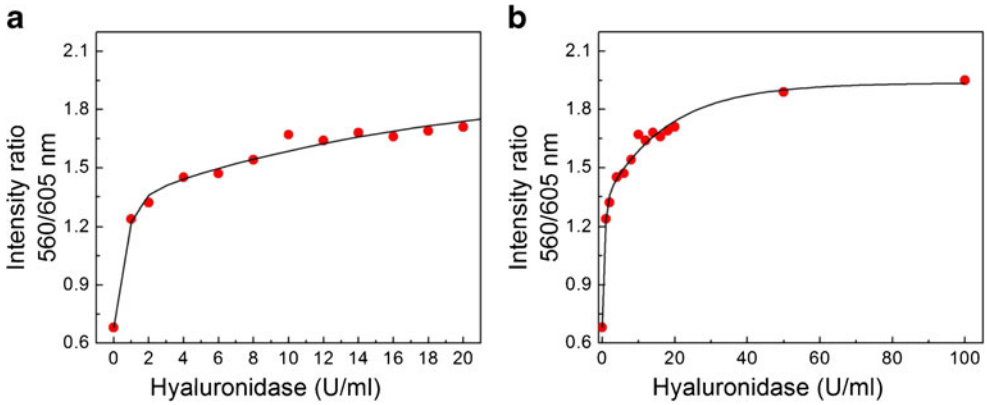

Fig. 5 The calibration curve for the intensity ratio of HA-ADOTA (70 nM ADOTA) probe in PBS (pH 7.4) at 100 min as a function of hyaluronidase levels (**A**) 0–20 U/mL and (**B**) 0–100 U/mL

as the end point in our experiment. Figure 5A represents the calibration curve obtained by measuring the change in the fluorescence intensity after 100 min as a function of hyaluronidase activity for enzyme within 0–20 U/mL, whereas Fig. 5B represents the entire region with 0–100 U/mL. Both the curves were fitted using exponential model ($Y = A_1 \times e^{(-X/t1)} + A_2 \times e^{(-X/t2)} + Y_o$, $R^2 = 0.98$). Details about the fitting method are given in the ESM. Using this standard curve, the level of hyaluronidase from an unknown sample can be easily determined.

Fluorescence lifetime-based sensing of hyaluronidase

We also desired to determine if the observed spectral changes are as well accompanied by the change in the fluorescence lifetime of the HA-ADOTA probe. The fluorescence intensity decay measurements are presented in Fig. 6 for HA-ADOTA probe in PBS at room temperature. The emission of the HA-ADOTA probe is highly quenched in the absence of hyaluronidase and shows a heterogenous decay. Three exponentials are needed to fit the data, and an amplitude-weighted lifetime of 4 ns is determined as compared to 20 ns lifetime for free fluorophore in PBS. In the presence of hyaluronidase, the amplitude-weighted lifetime increases with the increasing amount of enzyme. Table 1 shows the detailed analysis of the intensity decay of HA-ADOTA probe with different concentrations of hyaluronidase (0, 1, 10, 50, and 100 U/mL). The recovered average amplitude-weighted lifetime of HA-ADOTA probe with 100 U/mL of hyaluronidase was 15 ns, and two components were needed to fit the decay with amplitudes of 0.74 and 0.26 and lifetime of 18.85 and 1.83 ns. Figure 7 shows the change in the amplitude-weighted fluorescence lifetime of HA-ADOTA probe with different amounts of enzyme. It can be observed from the graph that with an increasing concentration of hyaluronidase and increasing time, an increase in the fluorescence lifetime is also observed. The time-resolved measurements demonstrate the generation of free unquenched ADOTA dyes ($\tau \sim 19$ ns) in the presence of hyaluronidase.

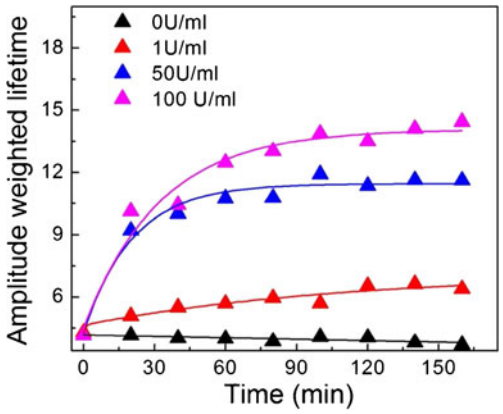

Fig. 7 The time-dependent change in the fluorescence lifetime of HA-ADOTA probe (70 nM ADOTA) in PBS (pH 7.4) in the absence and presence of hyaluronidase

Estimating hyaluronidase activity in cell culture media

It has been previously reported that several prostate cancer cell lines overexpress hyaluronidase activity. DU-145 is one such cell line which is reported to have overexpression of hyaluronidase. To investigate the activity of hyaluronidase produced by DU-145 prostate cancer cell line, we measured enzyme activity in concentrated serum-free culture media using an HA-ADOTA probe. In a solution of 100 μL of concentrated media and PBS (pH 7.4), HA-ADOTA probe (70 nM ADOTA in assay system) was added (total volume 1000 μL). The change in fluorescence intensity ratio was calculated every 10 min for 150 min (Fig. 8). The intensity ratio at 100 min was used to estimate hyaluronidase level using the standard curve obtained from spiked PBS buffer solution (Fig. 5). The calculated hyaluronidase level was 5 U/mL. To confirm if the fluorescence enhancement was caused by hyaluronidase, the effect of apigenin (inhibitor of hyaluronidase) was also examined on the activity of hyaluronidase [5, 55, 56]. Stock solution (20 mM) of apigenin was prepared in DMSO. The final concentration of apigenin in experimental solution was 50 μM. It was observed that the apigenin inhibited the fluorescence enhancement of HA-ADOTA probe. To confirm our steady-state fluorescence intensity data, we also measured the change in

Table 1 Amplitude-weighted lifetime of HA-ADOTA with different amount of hyaluronidase

Hyaluronidase concentration (U)	Time (min)								
	0	20	40	60	80	100	120	140	160
0	4.16 ns	4.16 ns	4.02 ns	4 ns	3.86 ns	4.08 ns	4.05 ns	3.8 ns	3.8 ns
1	4.3 ns	5.09 ns	5.51 ns	5.69 ns	6.07 ns	8.35 ns	8.63 ns	8.77 ns	8.89 ns
50	4.16 ns	9.22 ns	10.03 ns	10.75 ns	10.78 ns	11.91 ns	11.36 ns	11.64 ns	11.62 ns
100	4.16 ns	10.13 ns	10.44 ns	12.47 ns	13.03 ns	13.88 ns	13.5 ns	14.11 ns	14.45 ns

Averaged amplitude-weighted lifetime of HA-ADOTA probe was estimated every 20 min of the enzymatic reaction

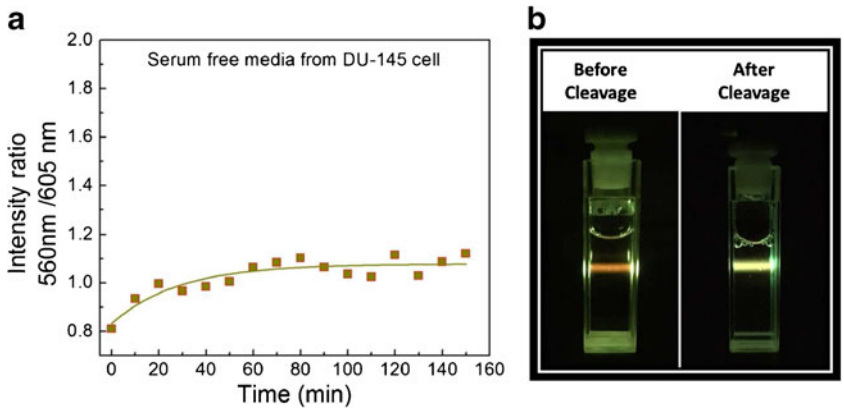

Fig. 8 (**A**) Change is the ratio of emission intensity (560 nm/605 nm) from cell culture media as a function of change in time. A 470-nm excitation was used and the reaction was continued for 150 min at room temperature. All the experiments were performed in triplicate. (**B**) Change in the color of fluorescence emission of HA-ADOTA probe in culture media before and after enzymatic cleavage

the fluorescence lifetime of HA-ADOTA probe in the concentrated serum-free media. Of concentrated media with PBS and HA-ADOTA probe (100 μL total volume), 10 μL was added to a glass bottom petri dish. Fluorescence lifetime was measured using a time-resolved microscope (MicroTime 200, PicoQuant, Germany). The main advantage of using confocal microscope with TCSPC abilities can help us to focus exactly at the center of the media while simultaneously only needing a small volume of the biological sample. The measured amplitude-weighted fluorescence lifetime of the undigested probe was around 4.5 ns. However, after 150 min of enzymatic reaction in the concentrated culture media, a fluorescence lifetime of 18 ns was measured. We also measured the effect of apigenin (hyaluronidase inhibitor) on the fluorescence lifetime of HA-ADOTA probe. Apigenin solution (50 μM) was prepared with 10 μL concentrated media and PBS (total volume = 100 μL). We found that the apigenin inhibited the activity of hyaluronidase and fluorescence lifetime of HA-ADOTA probe stayed constant (4.5 ns). These data suggest that the increase in fluorescence intensity and fluorescence lifetime indeed arises from the hyaluronidase activity. The amplitude-weighted fluorescence lifetime of HA-ADOTA probe in concentrated media with and without apigenin is given in Table 2.

Table 2 Amplitude-weighted fluorescence lifetime of HA-ADOTA probe media collected from DU-145 cell line

Time (min) apigenin	DU-145 media	DU-145 media with apigenin
Background	2.56 ns	2.07 ns
10	4.81 ns	2.8 ns
20	11.09 ns	4.3 ns
30	13.97 ns	5.1 ns
40	14.93 ns	4.14 ns
50	15.25 ns	5.28 ns
60	16.35 ns	3.48 ns
70	18.13 ns	4.56 ns
80	17.74 ns	5.24 ns
90	18.21 ns	4.03 ns
100	17.74 ns	3.85 ns
110	18 ns	4.28 ns
120	17.72 ns	4.3 ns
130	18.37 ns	4.12 ns
140	17.94 ns	4.78 ns
150	17.9 ns	4.87 ns

Data also shows the effect of apigenin on the inhibition of hyaluronidase activity from culture media

Conclusions

In summary, we have successfully developed a biosensor for hyaluronidase using an orange/red-emitting organic ADOTA fluorophore with a long fluorescence lifetime. This probe serves as an intensity-based ratiometric sensor and fluorescence lifetime-based sensor of hyaluronidase. Moreover, due to ratiometric sensing ability, a higher sensitivity can be achieved. The change in color of the fluorescence emission of undigested (red) and digested (yellow) HA-ADOTA probe can also be observed by the naked eyes using an appropriate excitation. Compared to other biosensors developed over nanoparticles, the biosensor developed using organic fluorophore is much smaller in size. The large difference between the fluorescence lifetime of undigested and digested probe helps to easily quantify hyaluronidase level using fluorescence lifetime as detection parameter. Emission in the orange/red region where there is a long fluorescence lifetime makes this probe highly useful for biological samples which possess a large amount of autofluorescence. It is a widely understood phenomenon that the contribution of autofluorescence decreases in the orange/red region of the electromagnetic spectrum. We successfully estimated the level of hyaluronidase in serum-free culture media of DU-145 prostate cancer cells. In conclusion, this HA-ADOTA biosensor can be easily used to measure hyaluronidase activity/level in complex pathological samples where the enzyme hyaluronidase is overexpressed.

Acknowledgments This work was supported by UNTHSC intramural grant RI6120 (R.F.), Sigma Xi grants in aid of research G20141015656984 (R.C.), UNTHSC pre-doctoral bridge grant RI6171 (R.C.), NIH grant R01EB12003 (Z.G.), and NSF grant CBET-1264608 (I.G.). We would like to thank Dr. Andras Lacko and Dr. Nirupama Sabnis for providing us the DU-145 cell line.

Compliance with ethical standards

Conflict of interest The authors declare that they have no competing interests.

References

1. Stern R. Hyaluronidases in cancer biology. Semin Cancer Biol. 2008;18(4):275–80.
2. Chao KL, Muthukumar L, Herzberg O. Structure of human hyaluronidase-1, a hyaluronan hydrolyzing enzyme involved in tumor growth and angiogenesis. Biochemistry (N Y). 2007;46(23):6911–20.
3. Bollet AJ, Bonner WM, Nance JL. The presence of hyaluronidase in various mammalian tissues. J Biol Chem. 1963;238:3522–7.
4. Franzmann EJ, Schroeder GL, Goodwin WJ, Weed DT, Fisher P, Lokeshwar VB. Expression of tumor markers hyaluronic acid and hyaluronidase (HYAL1) in head and neck tumors. Int J Cancer. 2003;106(3):438–45.
5. Liu D, Pearlman E, Diaconu E, Guo K, Mori H, Haqqi T, et al. Expression of hyaluronidase by tumor cells induces angiogenesis in vivo. Proc Natl Acad Sci U S A. 1996;93(15):7832–7.
6. Lokeshwar VB, Estrella V, Lopez L, Kramer M, Gomez P, Soloway MS, et al. HYAL1-v1, an alternatively spliced variant of HYAL1 hyaluronidase: a negative regulator of bladder cancer. Cancer Res. 2006;66(23):11219–27.
7. Chain E, Duthie E. Identity of hyaluronidase and spreading factor. Br J Exp Pathol. 1940;21(6):324.
8. Hobby GL, Dawson MH, Meyer K, Chaffee E. The relationship between spreading factor and hyaluronidase. J Exp Med. 1941;73(1):109–23.
9. McCUTCHEON M, COMAN DR. Spreading factor in human carcinomas. Cancer Res. 1947;7(6):379–82.
10. Turley EA, Noble PW, Bourguignon LY. Signaling properties of hyaluronan receptors. J Biol Chem. 2002;277(7):4589–92.
11. Girish K, Kemparaju K. The magic glue hyaluronan and its eraser hyaluronidase: a biological overview. Life Sci. 2007;80(21):1921–43.
12. Stern R. Hyaluronan catabolism: a new metabolic pathway. Eur J Cell Biol. 2004;83(7):317–25.
13. Stern R. Hyaluronan metabolism: a major paradox in cancer biology. Pathol Biol. 2005;53(7):372–82.
14. Stern R, Asari AA, Sugahara KN. Hyaluronan fragments: an information-rich system. Eur J Cell Biol. 2006;85(8):699–715.
15. Lokeshwar VB, Rubinowicz D, Schroeder GL, Forgacs E, Minna JD, Block NL, et al. Stromal and epithelial expression of tumor markers hyaluronic acid and HYAL1 hyaluronidase in prostate cancer. J Biol Chem. 2001;276(15):11922–32.
16. DORFMAN A, OTT ML. A turbidimetric method for the assay of hyaluronidase. J Biol Chem. 1948;172(2):367–75.
17. Knudsen P, Koefoed J. Viscometric determination of hyaluronidase activity in biological fluids. Scand J Clin Lab Invest. 1961;13(4):673–82.
18. Stern M, Stern R. An ELISA-like assay for hyaluronidase and hyaluronidase inhibitors. Matrix. 1992;12(5):397–403.
19. Pham HT, Block NL, Lokeshwar VB. Tumor-derived hyaluronidase: a diagnostic urine marker for high-grade bladder cancer. Cancer Res. 1997;57(4):778–83.
20. Bonner W, Cantey EY. Colorimetric method for determination of serum hyaluronidase activity. Clin Chim Acta. 1966;13(6):746–52.
21. Steiner B, Cruce D. A zymographic assay for detection of hyaluronidase activity on polyacrylamide gels and its application to enzymatic activity found in bacteria. Anal Biochem. 1992;200(2):405–10.
22. Podyma KA, Yamagata S, Sakata K, Yamagata T. Difference of hyaluronidase produced by human tumor cell lines with hyaluronidase present in human serum as revealed by zymography. Biochem Biophys Res Commun. 1997;241(2):446–52.
23. Cheng D, Han W, Yang K, Song Y, Jiang M, Song E. One-step facile synthesis of hyaluronic acid functionalized fluorescent gold nanoprobes sensitive to hyaluronidase in urine specimen from bladder cancer patients. Talanta. 2014;130:408–14.
24. Chib R, Raut S, Fudala R, Chang A, Mummert M, Rich R, et al. FRET based ratio-metric sensing of hyaluronidase in synthetic urine as a biomarker for bladder and prostate cancer. Curr Pharm Biotechnol. 2013;14(4):470–4.
25. Fudala R, Mummert ME, Gryczynski Z, Rich R, Borejdo J, Gryczynski I. Lifetime-based sensing of the hyaluronidase using fluorescein labeled hyaluronic acid. J Photochem Photobiol B Biol. 2012;106:69–73.
26. Huang Y, Song C, Li H, Zhang R, Jiang R, Liu X, et al. Cationic conjugated polymer/hyaluronan-doxorubicin complex for sensitive fluorescence detection of hyaluronidase and tumor-targeting drug delivery and imaging. ACS Appl Mater Interfaces. 2015;7(38):21529–37.
27. Liu S, Zhao N, Cheng Z, Liu H. Amino-functionalized green fluorescent carbon dots as surface energy transfer biosensors for hyaluronidase. Nanoscale. 2015;7(15):6836–42.
28. Murai T, Kawashima H. A simple assay for hyaluronidase activity using fluorescence polarization. Biochem Biophys Res Commun. 2008;376(3):620–4.
29. Wang Z, Li X, Song Y, Li L, Shi W, Ma H. An upconversion luminescence nanoprobe for the ultrasensitive detection of hyaluronidase. Anal Chem. 2015;87(11):5816–23.
30. Rich RM, Mummert M, Foldes-Papp Z, Gryczynski Z, Borejdo J, Gryczynski I, et al. Detection of hyaluronidase activity using fluorescein labeled hyaluronic acid and fluorescence correlation spectroscopy. J Photochem Photobiol B Biol. 2012;116:7–12.
31. Fudala R, Mummert ME, Gryczynski Z, Gryczynski I. Fluorescence detection of hyaluronidase. J Photochem Photobiol B Biol. 2011;104(3):473–7.
32. Hu Q, Zeng F, Wu S. A ratiometric fluorescent probe for hyaluronidase detection via hyaluronan-induced formation of red-light emitting excimers. Biosens Bioelectron. 2016;79:776–83.
33. Song Y, Wang Z, Li L, Shi W, Li X, Ma H. Gold nanoparticles functionalized with cresyl violet and porphyrin via hyaluronic acid for targeted cell imaging and phototherapy. Chem Commun. 2014;50(99):15696–8.
34. Wang W, Cameron AG, Ke S. Developing fluorescent hyaluronan analogs for hyaluronan studies. Molecules. 2012;17(2):1520–34.
35. Zhang L, Mummert ME. Development of a fluorescent substrate to measure hyaluronidase activity. Anal Biochem. 2008;379(1):80–5.
36. Xie H, Zeng F, Wu S. Ratiometric fluorescent biosensor for hyaluronidase with hyaluronan as both nanoparticle scaffold and substrate for enzymatic reaction. Biomacromolecules. 2014;15(9):3383–9.
37. Huang C, Chiang C, Lin Z, Lee K, Chang H. Bioconjugated gold nanodots and nanoparticles for protein assays based on photoluminescence quenching. Anal Chem. 2008;80(5):1497–504.

38. Chib R, Raut S, Shah S, Grobelna B, Akopova I, Rich R, et al. Steady state and time resolved fluorescence studies of azadioxatriangulenium (ADOTA) fluorophore in silica and PVA thin films. Dyes Pigments. 2015;117:16–23.
39. Folmar M, Shtoyko T, Fudala R, Akopova I, Gryczynski Z, Raut S, et al. Metal enhanced fluorescence of Me-ADOTA Cl dye by silver triangular nanoprisms on a gold film. Chem Phys Lett. 2012;531: 126–31.
40. Laursen BW, Sørensen TJ. Synthesis of super stable triangulenium dye. J Org Chem. 2009;74(8):3183–5.
41. Maliwal BP, Fudala R, Raut S, Kokate R, Sørensen TJ, Laursen BW, et al. Long-lived bright red emitting azaoxa-triangulenium fluorophores. Plos one. 2013;8(5):0063043.
42. Shtoyko T, Raut S, Rich RM, Sronce RJ, Fudala R, Mason RN, et al. Preparation of plasmonic platforms of silver wires on gold mirrors and their application to surface enhanced fluorescence. ACS Appl Mater Interfaces. 2014;6(21):18780–7.
43. Sørensen TJ, Laursen BW, Luchowski R, Shtoyko T, Akopova I, Gryczynski Z, et al. Enhanced fluorescence emission of Me-ADOTA by self-assembled silver nanoparticles on a gold film. Chem Phys Lett. 2009;476(1):46–50.
44. Sørensen TJ, Thyrhaug E, Szabelski M, Luchowski R, Gryczynski I, Gryczynski Z, et al. Azadioxatriangulenium: a long fluorescence lifetime fluorophore for large biomolecule binding assay. Methods Appl Fluoresc. 2013;1(2):025001.
45. Raut SL, Rich R, Shtoyko T, Bora I, Laursen BW, Sørensen TJ, et al. Sandwich type plasmonic platform for MEF using silver fractals. Nanoscale. 2015;7(42):17729–34.
46. Bogh SA, Bora I, Rosenberg M, Thyrhaug E, Laursen BW, Sørensen TJ. Azadioxatriangulenium: exploring the effect of a 20 ns fluorescence lifetime in fluorescence anisotropy measurements. Methods Appl Fluoresc. 2015;3(4):045001.
47. Laursen BW, Krebs FC. Synthesis, structure, and properties of azatriangulenium salts. Chem-A Eur J. 2001;7(8):1773–83.
48. Bora I, Bogh SA, Santella M, Rosenberg M, Sørensen TJ, Laursen BW. Azadioxatriangulenium: synthesis and photophysical properties of reactive dyes for bioconjugation. Eur J Organ Chem. 2015: 6351–6358.
49. Deng Y, Feng X, Zhou M, Qian Y, Yu H, Qiu X. Investigation of aggregation and assembly of alkali lignin using iodine as a probe. Biomacromolecules. 2011;12(4):1116–25.
50. Guo Z, Park S, Yoon J, Shin I. Recent progress in the development of near-infrared fluorescent probes for bioimaging applications. Chem Soc Rev. 2014;43(1):16–29.
51. Ajayaghosh A, Carol P, Sreejith S. A ratiometric fluorescence probe for selective visual sensing of Zn2. J Am Chem Soc. 2005;127(43): 14962–3.
52. Fan J, Hu M, Zhan P, Peng X. Energy transfer cassettes based on organic fluorophores: construction and applications in ratiometric sensing. Chem Soc Rev. 2013;42(1):29–43.
53. Niu L, Guan Y, Chen Y, Wu L, Tung C, Yang Q. BODIPY-based ratiometric fluorescent sensor for highly selective detection of glutathione over cysteine and homocysteine. J Am Chem Soc. 2012;134(46):18928–31.
54. Lokeshwar VB, Lokeshwar BL, Pham HT, Block NL. Association of elevated levels of hyaluronidase, a matrix-degrading enzyme, with prostate cancer progression. Cancer Res. 1996;56(3):651–7.
55. Kuppusamy U, Das N. Inhibitory effects of flavonoids on several venom hyaluronidases. Experientia. 1991;47(11–12):1196–200.
56. Tung J, Mark GE, Hollis GF. A microplate assay for hyaluronidase and hyaluronidase inhibitors. Anal Biochem. 1994;223(1):149–52.